RSC Advances

ROYAL SOCIETY
OF CHEMISTRY

www.rsc.org/advances

Graphical Abstract
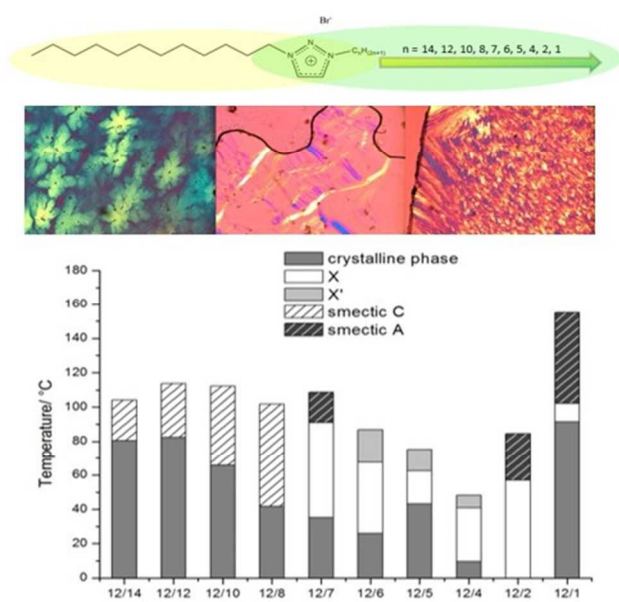
A new series of asymmetrical 1-dodecyl-3-alkyl-triazolium bromides has been synthesized to investigated effect of asymmetric substitution on their phase behavior.

Journal Name

ARTICLE

Triazolium Based Ionic Liquid Crystals: Effect of Asymmetric Substitution

K. Stappert[a] and A.-V. Mudring*[b]

A new series of ten different asymmetrical 1-dodecyl-3-alkyl-triazolium bromides, [C12CnTr][Br], has been synthesized and their mesomorphic behavior studied by DSC (differential scanning calorimetry), POM (polarizing optical microscopy) and SAXS (small angle X-ray scattering). The influence of the chain length of the triazolium salts is investigated to explore the effect of asymmetric substitution on the phase behaviour of these compounds. For that reason, the length of one alkyl chain was varied from 14 to 1 carbon atoms (n= 14, 12, 10, 8 – 4, 2, 1) while the other alkyl chain was kept at 12 carbons. Single crystal X-ray structure analysis of compounds [C12C12Tr][Br] and [C12C5Tr][Br] reveal that the cations adopt an U-shaped conformation with head-to-head arranged triazolium cores. In contrast, for [C12C1Tr][Br], a rod like shape of the cation with interdigitated alkyl chains is found. All investigated compounds are thermotropic liquid crystals. Higher ordered smectic phases, smectic C as well as smectic A phases were found depending on the chain length of the cation. Overall the clearing point temperature decreases with decreasing chain length with exception for the n-dodecyl-3-alkyltrizoliumbromides with the two shortest alkyl chains, [C12C2Tr][Br] and [C12C1Tr][Br], which present higher clearing temperatures (86 and 156 °C) and are structurally distinctly different..

Introduction

Ionic liquid crystals (ILCs) combine the properties of ionic liquids (ILs) and liquid crystals (LCs). ILs, salts with a melting point below 100 °C[1], usually consist of large organic cations and weakly coordinating anions. Due to their unique chemical and physical properties, such as low vapour pressure, thermal stability, electric conductivity and large electrochemical window they are of particular importance for several applications[2]. The variation of the cation or anion and the cation-anion combinations provide the possibility to tune the ionic liquid and its properties to fit to the applications needs[3,4]. Ionic liquids are, for example, used as alternative solvents[5], for nanomaterial synthesis, [6] as electrolytes in dye sensitised solar cells[7] or for the electrodeposition of metals[8]. Ionic liquids with mesogenic functionalities can exhibit thermotropic liquid crystalline phases[9]. Hence the ionic liquids characteristics are supplemented by anisotropy: various properties of this ionic liquid crystals depend on the directions. The ionic character in ILCs favors the formation of layered, smectic or even more highly ordered exotic phases.[9,10] Among the numerous cationic head groups, e.g. ammonium[11], imidazolium[12,13], morpholinium[14], pyrrolidinium[15,16], piperidinium14 and phosphonium[17], used for ILCs, the imidazolium based cations are the most studied ones. 1-Alkyl-3-methylimidazolium salts with long alkyl chains12,13 and bicationic imidazolium based salts[18,19,20] have been intensely analyzed. The influence of the the alkyl chain length of this cations on the mesogenic properties[21,22,23] and the role of the anion was investigated for different imidazolium based ILs and ILCs.2,[24,25,26] They can become magnetic or luminescent materials by making metal ions an integral part of the ILC. [27]

Typical application of ILCs is their use as an electrolyte in dye sensitized solar cells[28] or as pre-organized ionic solvents in catalysis[29]. The acidic imidazolium proton at C2 can cause problems in certain applications. In presence of bases, imidazolium cations can be deprotonated and stable carbenes are formed, inhibiting the desired reaction and favoring side reactions[30]. To circumvent deprotonation at the imidazolium C-2 position under basic conditions and decomposition of the ionic liquid, inert 1,2,3-triazolium based ionic liquids have been developed.[31] With the aim of answering what happens to the mesophase if we abstain from the acidic proton and replace the imidazolium by 1,2,3-triazolium, we recently reported on a set

of different new ILCs based on the symmetrical triazolium cation, in which the acidic CH group is

Table 1. Compound numbering scheme.

Nr.	1	2	3	4	5	6	7	8	9	10
	$[C_{12}C_{14}Tr][Br]$	$[C_{12}C_{12}Tr][Br]$	$[C_{12}C_{10}Tr][Br]$	$[C_{12}C_8Tr][Br]$	$[C_{12}C_7Tr][Br]$	$[C_{12}C_6Tr][Br]$	$[C_{12}C_5Tr][Br]$	$[C_{12}C_4Tr][Br]$	$[C_{12}C_2Tr][Br]$	$[C_{12}C_1Tr][Br]$
n	14	12	10	8	7	6	5	4	2	1

replaced by a nitrogen atom[32]. The absence of the acidic proton leads to different thermal behavior and to the formation of different mesophases. This highlights the influence of hydrogen bonding interactions upon the mesophase behavior. For further investigations, we expand our study of triazolium based ionic liquid crystals to asymmetric cations. In order to find out which minimal chain length is needed for the formation of a mesophase and what is the implication of symmetry, we synthesized a series of ten different 1-dodecyl-3-alkyl-triazolium bromide salts (Table 1) with one side chain of twelve carbon atoms and a variable number of carbons on the other side (Figure 1).
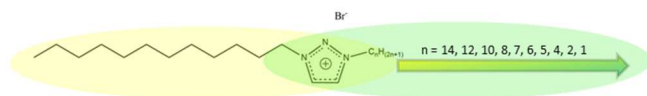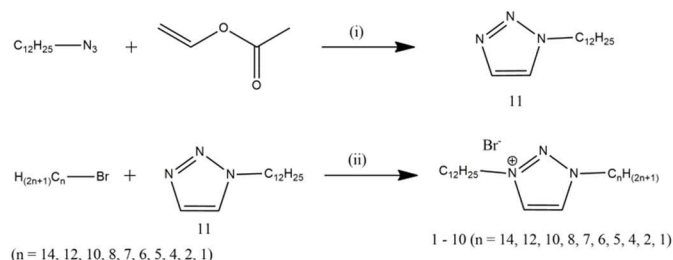
A common problem both in ionic liquid and liquid crystal chemistry is the growth of single crystals of sufficient quality for X-ray structure analysis since crystallization is frequently hindered kinetically.[33] Single crystals of 1,3-didodecyl-1,2,3-triazolium bromide ($[C_{12}C_{12}Tr][Br]$, (**2**)) and 1-dodecyl-3-methyl-1,2,3-triazolium bromide ($[C_{12}C_1Tr][Br]$, (**10**)) could be grown successfully from a dichloromethane solution. It was not possible to grow

single crystals of sufficient quality for structure analysis from solution, but single crystals of ($[C_{12}C_5Tr][Br]$) (**7**) could be grown successfully from its melt through a careful cooling procedure.

Figure 1. General structure of the synthesized compounds.

Results and Discussion

Synthesis

To obtain the different triazolium salts, dodecylazide was reacted with an excess of vinyl acetate to give 1-dodecyl-1,2,3-triazole (**11**) (Scheme 1). **11** was then alkylated at the N-3 position with the respective alkylbromide to give the different desired triazolium bromides (**1-10**). All compounds were obtained as slightly yellow solids. In contrast to the respective imidazolium salts which are highly hygroscopic[1,13], astonishingly none of the produced substances is air sensitive or hygroscopic. Thus, no protective atmosphere is required for the synthesis.

Scheme 1. Syntheses of triazolium compounds **1-10**. i) vinylacetate, 80 °C, 3 days; ii) acetonitrile, reflux, 3 days.

Structural Analysis

Table 2. Crystallographic and refinement details for compounds **2**, **7** and **10**.

	[C$_{12}$C$_{12}$Tr][Br] (**2**)	[C$_{12}$C$_5$Tr][Br] (**7**)	[C$_{12}$C$_1$Tr][Br] (**10**)
Empirical formula	C$_{26}$H$_{52}$N$_3$Br	C$_{19}$H$_{38}$N$_3$Br	C$_{15}$H$_{30}$N$_3$Br
Formular weight [g/mol]	468	388.4	332.3
Temperature [K]	170	170	170
Crystal system	triclinic	triclinic	triclinic
Space group	$P\bar{1}$	$P\bar{1}$	$P\bar{1}$
Unit cell dimensions	a = 4.916(5) Å b = 8.380(9) Å c = 35.58(4) Å α = 86.97(3) ° β = 87.29(3) ° γ = 75.07(3) °	a = 5.4919(9) Å b = 8.7562(16) Å c = 23.6945(46) Å α = 85.923(22) ° β = 88.179(22) ° γ = 82.518(20) °	a = 5.4934(17) Å b = 8.7114(15) Å c = 19.5010(50) Å α = 78.910(20) ° β = 85.390(30) ° γ = 84.046(17) °
Volume	1413(3)	1126.57(35)	909.11(42)
Z	2	2	2
Calculated density [g/cm^3]	1.14	1.14	1.21
Absorption coefficient [mm^{-1}]	1.470	1.829	2.255
Θ-range for data collection	1.15 to 25.00 °	2.5 to 25.00 °	2.4 to 25.00 °
Reflections collected/ unique	4289 / 2410	9043 / 3659	8375 / 3033
Refinement method	Full-matrix least-squares on F2		
Data / parameters	2410 / 273	3659 / 208	3033 / 174
Goodness-of-fit on F^2	1.008	1.474	0.901
Final R indices [I>2sigma(I)]	R$_1$ = 0.0699 wR$_2$ = 0.1392	R$_1$ = 0.184 wR$_2$ = 0.484	R$_1$ = 0.034 wR$_2$ = 0.076
R indices (all data)	R$_1$ = 0.1361 wR$_2$ = 0.2091	R$_1$ = 0.245 wR$_2$ = 0.484	R$_1$ = 0.048 wR$_2$ = 0.080

[C$_{12}$C$_{12}$Tr][Br] (**2**) crystallizes in the triclinic space group $P\bar{1}$ (No. 2) with two formula units in the unit cell. The two alkyl chains of one cation point in the same direction with respect to the triazolium head group and run nearly parallel leading to U-shaped cationic entities. The conformation of the alkyl chain is *all trans* except the bond from the first to the second carbon of the chain which is *gauche*. This allows the bromide anions to build hydrogen bonds to the first carbon-H of the chain. In addition, the two CH-groups of the triazolium ring also form C-H•••Br hydrogen bonds to (different) bromide anions (Table 3). Hence one bromide anion is connected via hydrogen bonds to three different cations (Figure 2). In the crystal, the cations form a bilayer structure with head-to-head arranged triazolium head groups (Figure 4). However, the triazolium cations are not facing each other directly but alternate with bromide anions. In contrast to many imidazolium ionic liquid crystals for which the crystal structure has been reported, the alkyl chains are not interdigitated. However, a clear structural segregation of

charged, polar domains made up by the triazolium head group and the hydrogen bonded bromide anions and the apolar, hydrophobic alkyl tails of the triazolium cation can be made out.
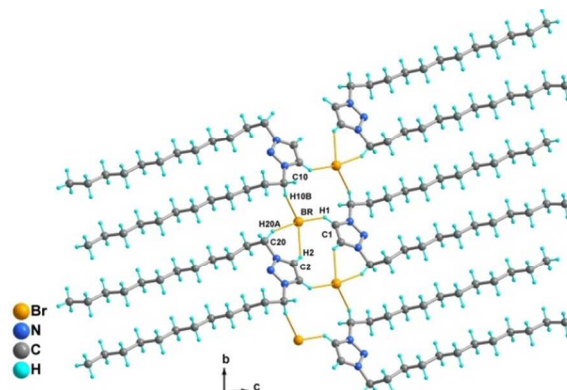
Figure 2. Hydrogen bonding interactions in **2**.
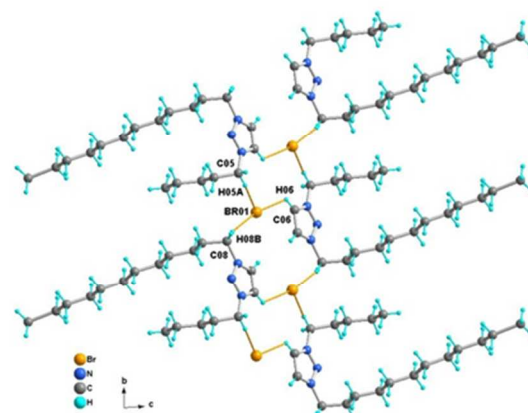
Figure 3. Hydrogen bonding interactions in **7**.

Table 3. H-bond details for compound **2** and **7**.

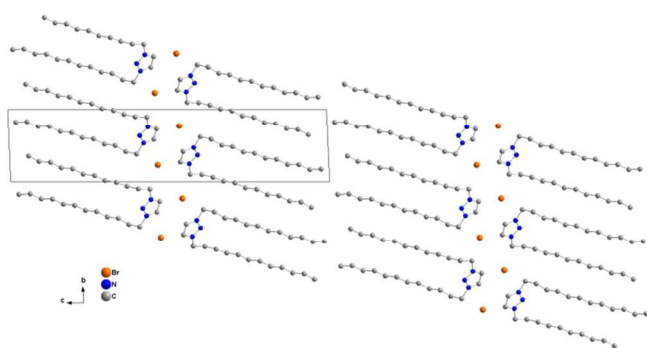| [C$_{12}$C$_{12}$Tr][Br]	H⋯A (Å)	H⋯A (deg)
C1-H1⋯Br	2.886(2)	126.27(8)
C2-H2⋯Br	2.908(3)	141.06(7)
C10-H10B⋯Br	2.874(2)	160.50(7)
C20-H20A⋯Br	2.824(2)	148.15(7)
[C$_{12}$C$_5$Tr][Br]		
C05-H05A⋯Br	2.846(3)	157.70(3)
C06-H06⋯Br	2.966(3)	122.56(2)
C08-H08B⋯Br	2.752(9)	165.67(2)

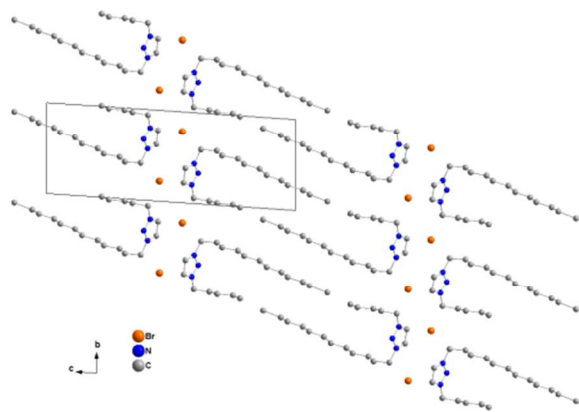Figure 4. Crystal packing of 1,3-didodecyl-triazolium bromide (**2**).

Figure 5. Crystal packing of 1-dodecyl-3-pentyl-triazolium bromide (**7**)

1-dodecyl-3-pentyl-triazolium bromide (**7**) crystalizes in the triclinic space group $P\overline{1}$ (No. 2) also with two formula units in the unit cell. Like [C$_{12}$C$_{12}$Tr][Br] (**2**) the cations adopt a U-shaped form with the alkyl chains almost parallel to each other. The alkyl chains are in *all trans* conformation except the bonds from the first to the second carbon of the chains which are gauche. This leads to similar hydrogen bonds as in the symmetric compound (**2**) (Figure 2 and 3). The bromide anion is bound via hydrogen bonds to three different cations. Two C-H•••Br hydrogen bonds connect the anion to the first carbon-Hs of the two different chains and the third hydrogen bond is built between the bromide anion and one CH-group of the triazolium ring (Table 3). The cations form a bilayer structure with the alkyl chains facing each other, whereby the long (twelve carbons) and the short (five carbons) alkyl chains alternate. The head-to-head arranged triazolium heads alternate with the bromide anions (Figure 5). The same structural segregation of charged, polar domains and the apolar, hydrophobic alkyltails as for the didodecyl-triazolium bromide can be found here.

In general both structures look very similar. A significant difference can be found in the angle between the triazolium head plane and the stretched alkyl chain. This angle is 43 ° for the symmetric compound (**2**) and 82 ° for the compound with two different alkyl chain lengths (**7**) (Figure 6). As a result of this the chains are almost perpendicular to the triazolium head

planes in **7**. In the crystal structure of the triazolium bromide with two alkyl chains of the same length (**2**) the triazolium heads are tilted towards the chains and the ring-carbons are facing each other. Here the distance between the carbons of two opposing triazolium rings is shorter than in the asymmetric compound (**7**) (3.9 Å vs. 4.6 Å).
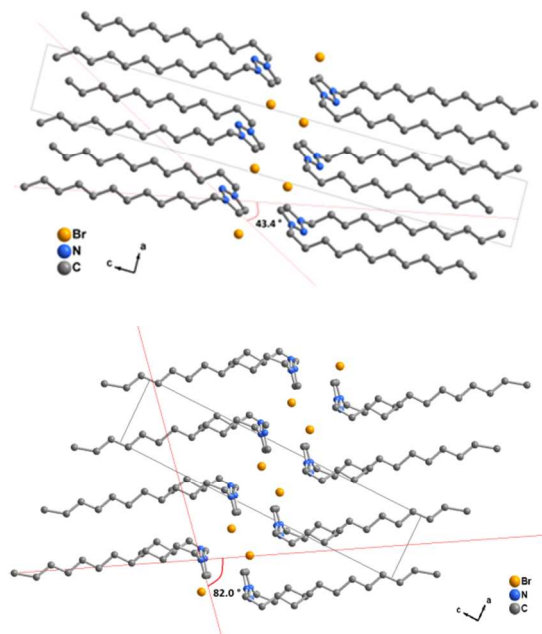
Figure 6. Comparison of parts of the crystal structure of 1,3-didodecyl-triazolium bromide (**2**, top) and 1-dodecyl-3-pentyl-triazolium bromide (**7**, bottom).

1-Dodecyl-3-methyl-1,2,3-triazolium bromide ([C$_{12}$C$_1$Tr][Br], (**10**)) crystallizes in the triclinic space group $P\overline{1}$ (No. 2) with two formula units in the unit cell. The cations adopt a rod-like shape with a tilted triazolium head, like a crank handle. The conformation of the alkyl chain is *all trans*. Hydrogen bonds are built between the bromide and two hydrogens of two different methyl groups (Figure 7). In addition, one CH-groups of the triazolium ring also form a C-H•••Br hydrogen bond to the bromide anions (Table 4). Again three different triazolium cations are connected via three C-H•••Br hydrogen bonds to one bromide anion.

The rod-shaped cations form an interdigitated bilayer-structure with the triazolium cations not facing each other directly but alternating with the bromide anions (Figure 8). The hydrophobic alkyl tails of the triazolium cation form apolar regions, which are clearly separated from the charged, polar domains made up by the triazolium head group and the hydrogen bonded bromide anions. In contrast to the U-shaped cations the alkyl chains are not perpendicular to the triazolium head plane but elongated. The angle between the methyl group at N3, the first carbon of the long chain at N1 and the methyl group at the end of the C$_{12}$-chain is larger than for the U-shaped cations (136 ° [C$_{12}$C$_1$Tr][Br] (**10**) vs. 84 ° [C$_{12}$C$_5$Tr][Br] (**7**) and 93 ° [C$_{12}$C$_{12}$Tr][Br] (**2**)).
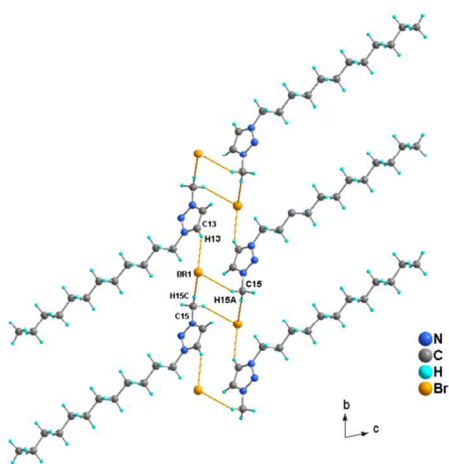
Figure 7. Hydrogen bonding interactions in **10**.
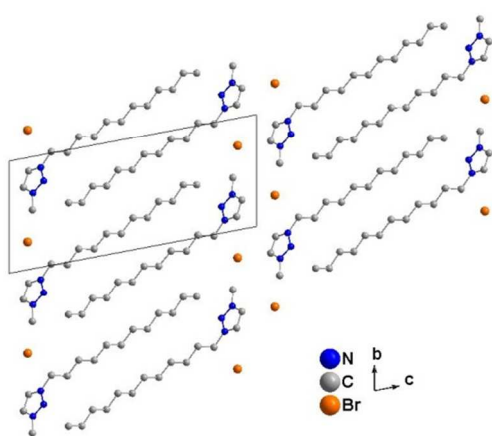
Figure 8. Crystal packing for 1-dodecyl-3-methyl-1,2,3-triazolium bromide (**10**).

Table 4. H-bond details for compound **10.**

[C$_{12}$C$_1$Tr][Br]	H···A (Å)	H···A (deg)
C13-H13···Br	2.8542(5)	144.238(33)
C15-H15A···Br	2.9194(8)	142.142(29)
C15-H15C···Br	2.8240(7)	172.54(3)

Thermal behaviour

The thermal properties of all compounds were examined by polarizing optical microscopy (POM) and differential scanning calorimetry (DSC). The transition temperatures, enthalpies and phase transition assignments are listed in Table 4. For the compounds with longer alkyl chains [C$_{12}$C$_{14}$Tr][Br] (**1**), [C$_{12}$C$_{12}$Tr][Br] (**2**), [C$_{12}$C$_{10}$Tr][Br] (**3**) and [C$_{12}$C$_8$Tr][Br] (**4**) two phase transitions were observed in the DSC (Figure 9). Temperature dependent POM identifies the first transition to be the flow point (S→LC) and the second one belongs to the clearing point (LC→L$_{ISO}$). All these transitions are reversible and reappear during cooling, albeit at slightly lower temperatures (due to kinetic inhibition of the phase transition) (Table 5).

Table 5. Phase transition temperatures of **1** to **10** and enthalpies (kJ/mol).

[C$_{12}$C$_{14}$Tr][Br] (1)

$$Cr \underset{69.3\,°C\,(31.86)}{\overset{80.5\,°C\,(27.73)}{\rightleftharpoons}} SmC \underset{97.9\,°C\,(16.97)}{\overset{104.0\,°C\,(10.69)}{\rightleftharpoons}} L$$

[C$_{12}$C$_{12}$Tr][Br] (2)

$$Cr \underset{22.4\,°C\,(1.3)}{\overset{30.5\,°C\,(4.06)}{\rightleftharpoons}} Cr' \underset{74.2\,°C\,(39.7)}{\overset{82.4\,°C\,(36.6)}{\rightleftharpoons}} SmC \underset{111.4\,°C\,(19.4)}{\overset{113.8\,°C\,(22.5)}{\rightleftharpoons}} L$$

[C$_{12}$C$_{10}$Tr][Br] (3)

$$Cr \underset{47.5\,°C\,(25.80)}{\overset{65.8\,°C\,(24.65)}{\rightleftharpoons}} SmC \underset{106.8\,°C\,(18.88)}{\overset{112.3\,°C\,(18.45)}{\rightleftharpoons}} L$$

[C$_{12}$C$_{8}$Tr][Br] (4)

$$Cr \underset{24.4\,°C\,(18.66)}{\overset{41.7\,°C\,(19.17)}{\rightleftharpoons}} SmC \underset{91.9\,°C\,(14.81)}{\overset{101.7\,°C\,(15.01)}{\rightleftharpoons}} L$$

[C$_{12}$C$_{7}$Tr][Br] (5)

$$Cr \underset{9.2\,°C\,(7.29)}{\overset{27.2\,°C\,(0.10)}{\rightleftharpoons}} Cr' \underset{23.3\,°C\,(9.02)}{\overset{35.2\,°C\,(15.17)}{\rightleftharpoons}} X \underset{83.4\,°C\,(6.35)\;88.9\,°C\,(18.66)}{\overset{91.0\,°C\,(5.16)}{\rightleftharpoons}} SmA \underset{99.0\,°C\,(0.29)}{\overset{108.6\,°C\,(0.23)}{\rightleftharpoons}} L$$

[C$_{12}$C$_{6}$Tr][Br] (6)

$$Cr \underset{-36.6\,°C\,(3.01)}{\overset{-0.7\,°C\,(4.13)}{\rightleftharpoons}} Cr' \underset{11.5\,°C\,(8.51)}{\overset{25.9\,°C\,(7.22)}{\rightleftharpoons}} X \underset{66.5\,°C\,(2.97)}{\overset{67.6\,°C\,(1.69)}{\rightleftharpoons}} X' \underset{84.6\,°C\,(2.08)}{\overset{86.9\,°C\,(2.14)}{\rightleftharpoons}} L$$

[C$_{12}$C$_{5}$Tr][Br] (7)

$$Cr \underset{25.2\,°C\,(8.09)}{\overset{43.1\,°C\,(4.77)}{\rightleftharpoons}} X \underset{55.2\,°C\,(4.26)}{\overset{62.6\,°C\,(1.87)}{\rightleftharpoons}} X' \underset{73.0\,°C\,(1.57)}{\overset{75.3\,°C\,(1.55)}{\rightleftharpoons}} L$$

[C$_{12}$C$_{4}$Tr][Br] (8)

$$Cr \underset{-7.8\,°C\,(4.16)}{\leftarrow} Cr' \underset{9.6\,°C\,(5.57)}{\leftarrow} X \underset{41.0\,°C\,(4.54)}{\leftarrow} X' \underset{48.3\,°C\,(0.52)}{\overset{51.7\,°C\,(12.72)}{\longrightarrow}} L$$

[C$_{12}$C$_{2}$Tr][Br] (9)

$$Cr \underset{-10.9\,°C\,(0.34)}{\overset{-8.4\,°C\,(0.24)}{\rightleftharpoons}} X \underset{34.7\,°C\,(22.09)}{\overset{57.1\,°C\,(15.93)}{\rightleftharpoons}} SmA \underset{82.8\,°C\,(0.65)}{\overset{84.6\,°C\,(0.53)}{\rightleftharpoons}} L$$

[C$_{12}$C$_{1}$Tr][Br] (10)

$$Cr \underset{-36.6\,°C\,(3.01)}{\overset{-0.7\,°C\,(4.13)}{\rightleftharpoons}} Cr' \underset{57.0\,°C\,(23.64)}{\overset{91.5\,°C\,(12.98)}{\rightleftharpoons}} X \overset{102.3\,°C\,(14.88)}{\longrightarrow} SmA \underset{143.5\,°C\,(0.59)}{\overset{156.0\,°C\,(0.84)}{\rightleftharpoons}} L$$

Sm A = smectic A, *smC* = smectic C, *X* and *X'* = higher ordered mesophases.

In addition the DSC traces of compound **2** show one additional thermal event at room temperature, which can be attributed to a solid–solid phase transition. For compounds **2** to **4** flow point- and clearing point-temperatures increase with increasing chain length (Figure 9). The increase of the alkyl chain to a length of 14 carbons leads to a decrease in phase transition temperatures. Compound **5** ([C$_{12}$C$_{7}$Tr][Br]) shows four phase transitions in total (Figure 9). The thermal change around room temperature is due to a solid-solid phase transition. The last transition (T = 110 °C) could be associated to the clearing point (LC→L$_{ISO}$). The thermal event at 90 °C belongs to a transition between two different liquid crystalline phases and accordingly the transition at 40 °C can be identified as the flow point (S→LC).

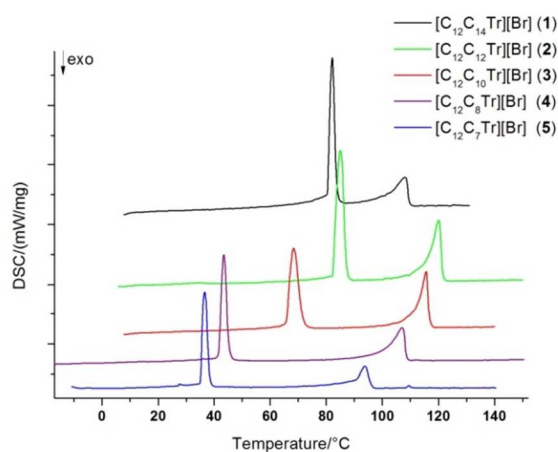The DSC-traces of compounds **6** to **8** can be seen in Figure 10. Here the cooling curves are presented because in the heating curve of compound **8** all thermal events are merged to one broad, featureless transition. Upon cooling the isotropic liquid of [C$_{12}$C$_{6}$Tr][Br] (**6**), [C$_{12}$C$_{5}$Tr][Br] (**7**) or [C$_{12}$C$_{4}$Tr][Br] (**8**) a mesophase occurs. During further cooling a transition to another more highly ordered mesophase takes place between 66 and 40 °C, followed by the transition to a crystalline phase at temperatures between 25 and 10 °C. Compound **6** and **8** undergo a solid-solid phase transition at temperatures below 0 °C (-37 °C, -8 °C respectively). The clearing points follow the same trend as the compounds **2** to **4**: temperature decreases with decreasing chain length (Figure 13). This tendency can also be found for the transition temperatures of the LC <-> LC' transition. No correlation of the alkyl chain length and the temperature of the flow point can be found here.

Figure 9. DSC-heating-traces of **1**, **2**, **3**, **4** and **5**.
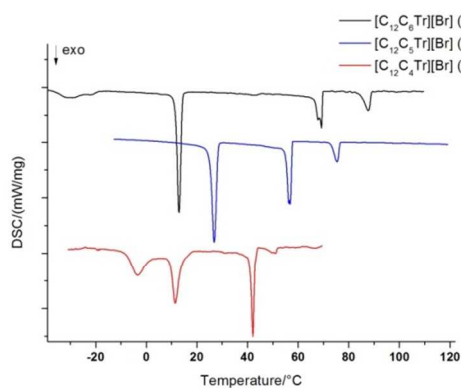

Figure 10. DSC-cooling-traces of **6**, **7** and **8**.

The DSC traces of compounds $[C_{12}C_2Tr][Br]$ (**9**) and $[C_{12}C_1Tr][Br]$ (**10**) show three phase transitions (Figure 11). Compound **9** exists in a more highly ordered mesophase (*X*) at room temperature. Crystallization occurs upon cooling around -10 °C. Upon heating compound **9** exhibits a liquid crystalline phase around 60 °C and melts into an isotropic liquid at 85 °C. This mesophase was identified with temperature dependent POM as a smectic A phase, which was also found for compound **10** during heating from 100 °C to 156 °C. Upon cooling the isotropic liquid the smectic A phase reappears and persists until the substance crystallizes at 57 °C. The additional thermal event below room temperature can be attributed to a solid–solid phase transition. The transition from the crystalline phase to the smectic A phase is split into two thermal events in the heating curve (Figure 11). The intermediate phase was not clearly identified, but is expected to be a more highly ordered mesophase.
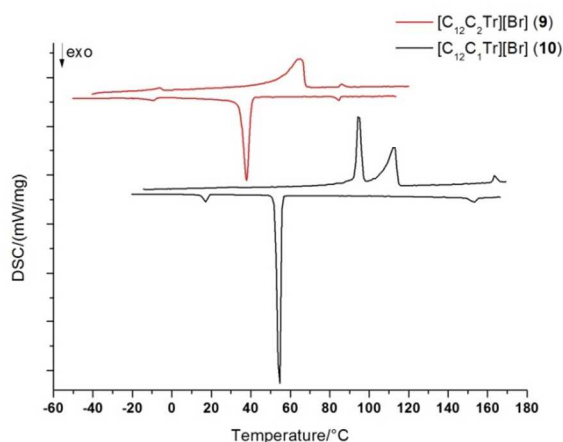

Figure 11. DSC-thermograms of **9** and **10**.

The identification of transition temperatures and the proof of mesophase formation was undertaken by POM (polarizing optical microscopy). Figure 12 shows some representative POM textures for observed mesophases obtained by heating and cooling of the compounds. The smectic A phases were recognized by the formation of oily streak textures and homeotropic domains (Figure 12b). No homeotropic alignment was observed for the smectic C phases (Figure 12c), but fan shaped textures were formed. For the higher ordered phases platelet textures suggest a smectic E phase (Figure 12a), but for an unambiguous assignment the textures are not clear enough.

Comparison of the phase transition temperatures of all ten compounds illustrates the dependency of the alkyl chain length (Figure 13). Starting with the symmetric di-dodecyl-triazolium bromide the flow point temperature and the clearing point temperature decrease with decreasing symmetric of the cation. When decreasing the chain length a decrease of the flow point temperature and the clearing point temperature is observed until a chain length of eight carbons is reached. When a chain length of seven carbons atoms is reached different phases are formed

which point that the subtle interpolate of geometric and weak interactions is changed, ($[C_{12}C_7Tr][Br]$ (**5**)). Upon further decreasing the carbon chain to four carbon atoms, the flow point and the clearing point temperatures are decreased. For the transition from the crystalline phase to the higher ordered mesophase no trend was observed. When the second chain is too short compared to the first one with twelve carbons, the molecular arrangement is totally changed, as seen in the crystal structure and the thermal behavior changes as well. The salts with an ethyl or methyl group on one side exhibit smectic A phases. Within these two compounds the transition temperatures increase with decreasing chain length.
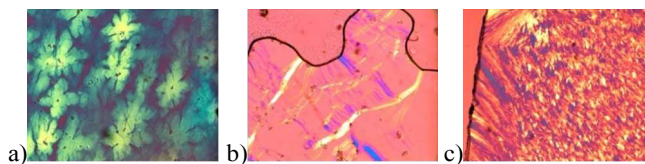

Figure 12. Representative textures as seen between crossed polarizers: a) higher ordered mesophase of **5** at 74.7 °C, b) SmA phase of **10** at 154.8 °C, c) SmC phase of **1** at 88.6 °C.
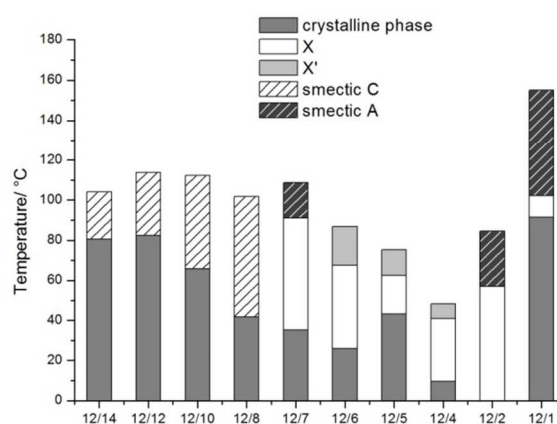

Figure 13. Phase transition temperatures of compounds **1**-**10** in dependency of the alkyl chain length.

Small Angle X-ray Scattering

To identify the mesophase and to comprehend the molecular arrangement of the triazolium salts temperature dependent SAXS measurements were carried out. All compounds display a similar SAXS pattern with one sharp peak between 2 and 3 ° corresponding to (001), hence, the interlayer distance of a layered phase, and in most cases smaller second order (002) and third order (003) peaks. Since these measurements do not include distances or peaks that appear below 12.2 Å, additional temperature dependent powder XRD (PXRD) measurements were carried out. A representative SAXS pattern and the corresponding PXRD pattern are displayed in Figure 14. The overlap of the measuring range can be seen on the (003) peak, which occurs in both diffractograms. This third order peak appears at s = 0.1016 Å^{-1} in the SAXS pattern and at 2Θ = 4.045 ° in the powder-XRD pattern (arrows in Figure 14). The other SAXS- and PXRD-patterns can be found in the

supporting information. The layer distances from the SAXS measurements, calculated from Bragg's law are listed in Table 6.
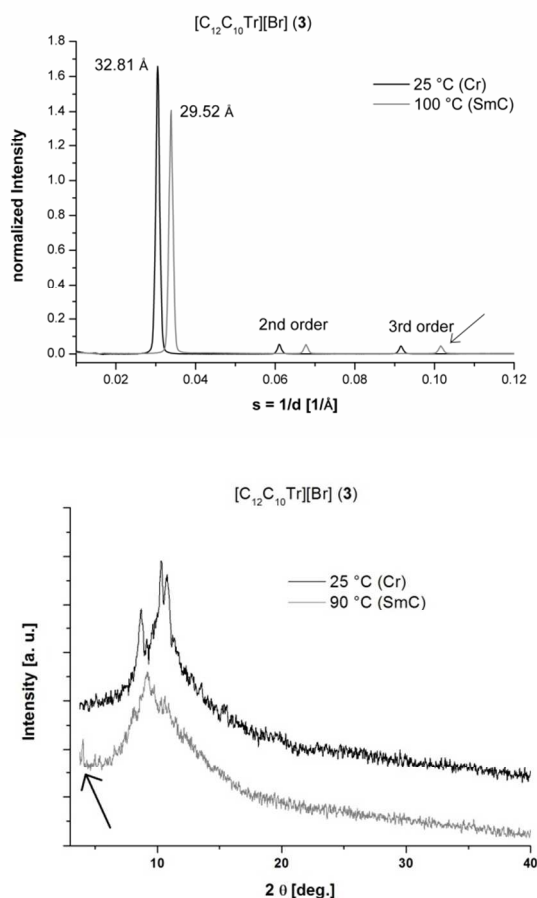

Figure 14. SAXS pattern (top) and PXRD pattern (bottom) of 1-dodecyl-3-decyl-1,2,3-triazolium bromide (**3**). The (003) peak is indicated by an arrow.

Table 6. Layer spacing (d, Å) of the triazolium salts in the different phases.

No.	Formula	crystal	X	X'	SmC	SmA
1	$[C_{12}C_{14}Tr][Br]$	37.8			33.8	
2	$[C_{12}C_{12}Tr][Br]$	35.3			31.6	
3	$[C_{12}C_{10}Tr][Br]$	32.8			29.5	
4	$[C_{12}C_8Tr][Br]$	30.4			27.6	
5	$[C_{12}C_7Tr][Br]$	29.5	26.1			26.3
6	$[C_{12}C_6Tr][Br]$	24.9	25.1	25.2		
7	$[C_{12}C_5Tr][Br]$	23.9	23.6	23.3		
8	$[C_{12}C_4Tr][Br]$	23.0	22.8	23.4		
9	$[C_{12}C_2Tr][Br]$	21.0				27.6
10	$[C_{12}C_1Tr][Br]$	19				28

The distance of 35 Å of compound **2** can be identified as the bilayer spacing in the crystal structure of this salt. This distance decreases proportionally with decreasing chain length (**1**: 37 Å, **2**: 35 Å, **3**: 33 Å, **4**:31) for the first four compounds. The layer distance decreases significantly by 3-4 Å in all four compounds (**1, 2, 3, 4**) when the phase transition to the mesophase occurs. The cations themselves supposedly keep their U-shaped conformation with end-to-end packing of the alkyl chains (Figure 15). The diffraction pattern of the mesophase with diffraction peaks with reciprocal spacing in the ratio 1:2:3 suggest a layered structure. A smectic C phase is assumed for this four salts, because no homeotropic alignment was observed under polarized light and the enthalpy changes for the transition to the isotropic liquid is larger than expected for a smectic A phase.
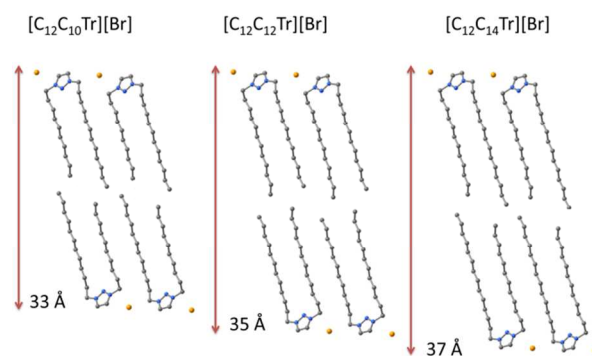

Figure 15. Schematic model of the molecular packing of compounds **1-3**.

The bilayer spacing in the crystal structure of compound **7** ($[C_{12}C_5Tr][Br]$) is confirmed by the SAXS-measurements. For the compounds **6** to **8** this distance decreases with decreasing chain length (**6**: 25 Å, **7**: 23.2 Å, **8**: 22.5)(Table 6). Hence a similar structure is assumed for the compounds **6** and **8** (Figure 16). Since for these substances no significant change in layer spacing was observed upon heating, no conclusion could be drawn concerning the mesophase identification. The powder-XRD diffractograms show more reflections for the phases observed in this compounds than observed for the smectic C or smectic A phases, so highly ordered smectic phases are assumed. The alkyl chains of different length hinder each other, thus the disorder is restrained and higher ordered phases are formed.
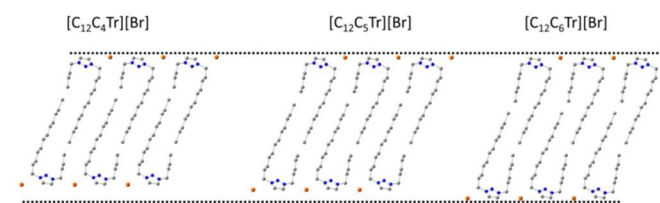

Figure 16. Structural representation of the molecular packing of compounds **6-8**.

The distance of 19 Å of compound **10** can be identified as the bilayer spacing in the crystal structure of this salt. For

compound **9** this distance is slightly large (20 Å), due to the ethyl group instead of the methyl group. For both compounds the layer spacing is significantly larger in the mesophase (7-9 Å). This is similar to what was observed for imidazolium based compounds of this kind[13]. The mesophase has been clearly identified by POM as smectic A phase. The increase in layer spacing can be attributed to alkyl chain melting and simultaneous decrease of interdigitation as shown schematically in Figure 17.
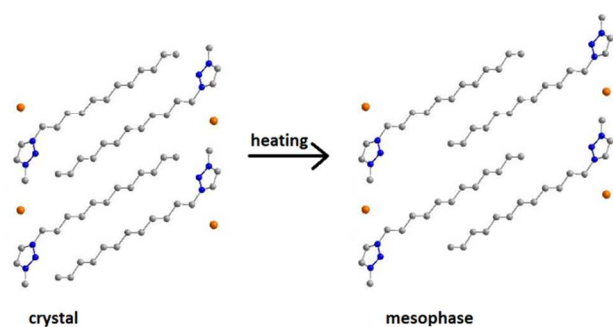

Figure 17. Schematic model of the smectic A phase of compound **10**.

Conclusion

A series of ten different new asymmetrical 1-dodecyl-3-alkyl-triazolium based ionic liquids with bromide anion has been synthesized. The alkyl chain length was varied systematically from 14 to 1 carbon units. The aim was to identify the influence of the cation chain length on the thermal behavior and to reveal the role of symmetry of the cation. The series of substances can be diveded into three main groups with similar thermal behavior. The first group ranges from $C_{14}H_{29}$ to C_8H_{17} (compounds **1-4**) Here, the cations adopt an U-shaped conformation and arrange in bilayers with separated polar and apolar regions. All four compounds exhibit a smectic C phase upon heating. The flow point temperature and the clearing point temperature decrease with decreasing chain length. This trend is interrupted when a heptyl chain is reached. Apparently the subtle interplay between size, van-der-Waals forces and hydrogen bonding and Coulombic forces is altered. The hydrophobic interactions of the alkyl chains compete against ionic interactions of the polar head groups. Increasing influence of Coulombic forces results in formation of a more highly ordered mesophase and a smectic A phase at higher temperatures for compound **5**, ($[C_{12}C_7Tr][Br]$). The next three compounds form another group with respect to their structural and thermal behaviour. Though the general constitution of the molecules is similar to those with longer chains (U-shape, bilayer) the thermal behaviour is different. $[C_{12}C_6Tr][Br]$ (**6**), $[C_{12}C_5Tr][Br]$ (**7**), and $[C_{12}C_4Tr][Br]$ (**8**) exhibit two different higher ordered mesophases and do not show a smectic A or C phase. The last two salts of the series ($[C_{12}C_2Tr][Br]$ (**9**) and $[C_{12}C_1Tr][Br]$ (**10**)) form another group as they behave totally

different. The U shape can no longer be adopted by the cation since the second alkyl chain is too short. In addition cation arrangement can be described as an interdigitated bilayer (interdigitation of the alkyl chains is not observed for the other compounds). Both compounds form a smectic A phase, though at considerably different temperatures (**9**: 85 °C, **10**: 156 °C). Compared to the analogous imidazolium and 2-methylimidazolium compound the phase transitions of $[C_{12}C_1Tr][Br]$ (**10**) occur at higher temperatures. [34] The imidazolium salt corresponding to compound **9** does not show a liquid crystalline phase but melts into an isotropic liquid below 40 °C. [35] It is incorrect or even misguiding to compare the other imidazolium salts with the corresponding triazolium salts, because of their fundamentally different structures. No U-shaped conformation was observed in their crystals structures or indicated by the layer distances for the respective imidazolium compounds. In summary, all synthesized triazolium based salts have higher melting points then the respective imidazolium bromides.

Experimental Section

Synthesis

The alkylazides were synthesized according to a common literature method[36]. All other starting materials and solvents were purchased from standard commercial sources and were used without further purification. No protective atmosphere was required during synthesis.

PREPARATION OF 1-DODECYL-1,2,3-TRIAZOLE (11)

5g dodecylazide (23.7 mmol) and 10 ml vinyl acetate were heated in a closed glass tube for three days. After addition of 200 ml n-hexane the suspension was filtered and the solution cooled to -40 °C for 24 hours. The precipitated product was filtered off and dried overnight in vacuum at room temperature.

1-DODECYL-1,2,3-TRIAZOLE (11).

Yield: 3.98 g (71 %), ^1H NMR (200 MHz, CDCl$_3$) δ: 7.69 (s, 1H), 7.52 (s, 1H), 4.38 (t, J = 7.2 Hz, 2H), 1.92 (dd, J = 12.4, 5.7 Hz, 2H), 1.25 (s, 18H), 0.88 (t, J = 6.3 Hz, 4H).

GENERAL PROCEDURE FOR THE PREPARATION OF 1-DODECYL-3-ALKYL-1,2,3-TRIAZOLIUM BROMIDES (1-10)

A solution of the 1-dodecyl-1,2,3-triazole (**11**) and four equivalents of the respective alkylbromide was heated under reflux in acetonitrile for three days. After cooling to room temperature the solution was poured into cold ethyl acetate and kept at -40 °C for 5 hours. The white precipitate was filtered off and dried under vacuum at room temperature to give the products in good yields and purity (80 – 85 %).

1-DODECYL-3-TETRADECYL-1,2,3-TRIAZOLIUM BROMIDE (1)

^1H NMR (200 MHz, CDCl$_3$) δ: 9.61 (s, 2H), 4.76 (t, J = 7.3 Hz, 4H), 2.05 (s, 4H), 1.39 – 1.22 (m, 40H), 0.88 (t, J = 6.4 Hz, 6H). ^{13}C NMR (50 MHz, CDCl$_3$) δ: 132.0, 54.6, 32.2, 29.9, 29.9, 29.8, 29.7, 29.2, 26.5, 23.0, 14.5. MS (FAB): m/z 70 (9 %, TrH$^+$), 434 (100 %, K$^+$), 949 (1.2 %, 2*K$^+$ + Br$^-$). Elemental

analysis (%) calcd for ($C_{28}H_{56}N_3Br$): C 65.34, H 10.97, N 8.16; found: C 64.88, H *11.04*, N 7.84.

1,3-didodecyl-1,2,3-triazolium bromide (2)
^{1}H NMR (200 MHz, $CDCl_3$) δ: 9.75 (s, 1H), 4.77 (t, J = 7.3 Hz, 2H), 2.14 – 1.93 (m, 2H), 1.41 – 1.09 (m, 18H), 0.87 (t, J = 6.4 Hz, 3H). ^{13}C NMR (50 MHz, $CDCl_3$) δ: 131.8, 54.3, 32.0, 29.7, 29.6, 29.6, 29.5, 29.4, 28.9, 28.3, 26.2, 22.8, 14.2. MS (FAB): m/z 406.2 (K^+), 893 (5 %, $2*K^+ + Br^-$). Elemental analysis (%) calcd for ($C_{26}H_{52}N_3Br$): C 64.17, H 10.77, N 8.64; found: C 63.96, H *11.27*, N 8.34.

1-dodecyl-3-decyl-1,2,3-triazolium bromide (3)
^{1}H NMR (200 MHz, $CDCl_3$) δ: 9.56 (s, 1H), 4.75 (t, J = 7.2 Hz, 2H), 2.14 – 1.95 (m, 2H), 1.39 – 1.19 (m, 16H), 0.88 (t, J = 5.8 Hz, 3H). ^{13}C NMR (50 MHz, $CDCl_3$) δ: 131.8, 54.3, 32.0, 31.9, 29.8, 29.7, 29.6, 29.5, 29.5, 29.4, 28.9, 26.3, 22.8, 14.2. MS (FAB): m/z 378 (100 %, K^+), 837 (1,1 %, $2*K^+ + Br^-$). Elemental analysis (%) calcd for ($C_{24}H_{48}N_3Br$): C 62.86, H 10.55, N 9.16; found: C 62.37, H 10.82 , N 8.91.

1-dodecyl-3-octyl-1,2,3-triazolium bromide (4)
^{1}H NMR (200 MHz, $CDCl_3$) δ: 9.63 (s, 2H), 4.76 (t, J = 7.2 Hz, 4H), 2.12 – 1.93 (m, 4H), 1.46 – 1.09 (m, 28H), 0.87 (t, J = 6.0 Hz, 6H). ^{13}C NMR (50 MHz, $CDCl_3$) δ: 131.8, 54.3, 32.0, 31.8, 29.8, 29.7, 29.6, 29.5, 29.1, 28.9, 28.9, 26.2, 22.8, 22.7, 14.2, 14.2. MS (FAB): m/z 70 (14 %, TrH^+), 350 (100 %, K^+),406 (6,6 % $K^+ - C_8H_{17} + C_{12}H_{25}$). Elemental analysis (%) calcd for ($C_{22}H_{44}N_3Br$): C 61.38, H 10.3, N 9.76; found: C 61.41, H 10.90, N 9.40.

1-DODECYL-3-HEPTYL-1,2,3-TRIAZOLIUM BROMIDE (5)
^{1}H NMR (200 MHz, $CDCl_3$) δ: 9.72 (s, 2H), 4.77 (t, J = 7.3 Hz, 4H), 2.03 (d, J = 6.6 Hz, 4H), 1.40 – 1.13 (m, 26H), 0.87 (t, J = 6.5 Hz, 6H). ^{13}C NMR (50 MHz, $CDCl_3$) δ: 131.8, 54.3, 32.0, 31.6, 29.8, 29.7, 29.6, 29.5, 28.9, 28.6, 26.3, 26.2, 22.8, 22.6, 14.2, 14.1. MS (FAB): m/z 70 (11 %, TrH^+), 336 (100 %, K^+), 406 (3.6 %, $C_{12}C_{12}Tr^+$). Elemental analysis (%) calcd for ($C_{21}H_{42}N_3Br$): C 60.56, H 10.16, N 10.09; found: C 60.30, H 10.57 , N 9.84.

1-DODECYL-3-HEXYL-1,2,3-TRIAZOLIUM BROMIDE (6)
^{1}H NMR (200 MHz, $CDCl_3$) δ: 9.74 (d, J = 1.8 Hz, 2H), 4.78 (t, J = 7.3 Hz, 4H), 2.12 – 1.94 (m, 4H), 1.28 (d, J = 15.7 Hz, 26H), 0.87 (t, J = 6.1 Hz, 6H). ^{13}C NMR (50 MHz, $CDCl_3$) δ: 131.8, 54.3, 32.0, 31.0, 29.8, 29.7, 29.7, 29.6, 29.4, 28.9, 26.2, 25.9, 22.8, 22. 4, 14.2, 14.0. MS (FAB): m/z 70 (9 %, TrH^+), 322 (100 %, K^+),406 (8 % $K^+ - C_6H_{13} + C_{12}H_{25}$), 725 (3 %, $2*K^+ + Br^-$). Elemental analysis (%) calcd for ($C_{20}H_{40}N_3Br$): C 59.69, H 10.02, N 10.44; found: C 59.70, H 10.00 , N 10.29.

1-DODECYL-3-PENTYL-1,2,3-TRIAZOLIUM BROMIDE (7)
^{1}H NMR (200 MHz, $CDCl_3$) δ: 9.74 (d, J = 3.5 Hz, 2H), 4.78 (dd, J = 10.6, 3.9 Hz, 4H), 2.02 (d, J = 6.4 Hz, 4H), 1.27 (d, J = 17.8 Hz, 22H), 0.86 (q, J = 6.2 Hz, 6H). ^{13}C NMR (50 MHz, $CDCl_3$) δ: 131.8, 131.7, 54.3, 32.0, 29. 8, 29.7, 29.6, 29.5, 29.4, 28.93, 28.2, 26.2, 22.8, 22.0, 14.2, 13.9. MS (FAB): m/z 70 (10 %, TrH^+), 308 (100 %, K^+), 406 (5.5 %, $C_{12}C_{12}Tr^+$). Elemental analysis (%) calcd for ($C_{19}H_{38}N_3Br$): C 58.75, H 9.86, N 10.82; found: C 58.77, H 10.59 , N 10.65.

1-DODECYL-3-BUTYL-1,2,3-TRIAZOLIUM BROMIDE (8)
^{1}H NMR (200 MHz, $CDCl_3$) δ: 9.73 (d, J = 8.0 Hz, 2H), 4.77 (dd, J = 11.4, 6.9 Hz, 4H), 2.00 (dd, J = 14.7, 7.1 Hz, 4H), 1.36 – 1.17 (m, 20H), 0.95 (t, J = 7.4 Hz, 3H), 0.84 (t, J = 6.0 Hz, 3H). ^{13}C NMR (50 MHz, $CDCl_3$) δ: 131.8, 131.8, 54.3, 54.0, 32.0, 31.7, 29.8, 29.7, 29.6, 29.4, 28.9, 26.2, 22.8, 19.5, 14.2, 13.4. MS (FAB): m/z 70 (8 %, TrH^+), 294 (100 %, K^+), 406 (9 % $K^+ - C_4H_9 + C_{12}H_{25}$), 669 (2,5 %, $2*K^+ + Br^-$). Elemental analysis (%) calcd for ($C_{18}H_{36}N_3Br$): C 57.74, H 9.69, N 11.22; found: C 58.32, H 10.53, N 10.95.

1-DODECYL-3-ETHYL-1,2,3-TRIAZOLIUM BROMIDE (9)
^{1}H NMR (200 MHz, $CDCl_3$) δ: 9.79 (s, 1H), 9.64 (s, 1H), 4.82 (dt, J = 24.5, 7.4 Hz, 4H), 2.13 – 1.98 (m, 2H), 1.72 (t, J = 7.4 Hz, 3H), 1.35 – 1.22 (m, 18H), 0.87 (t, J = 5.9 Hz, 3H). ^{13}C NMR (50 MHz, $CDCl_3$) δ: 131.7, 131.6, 54.4, 49.8, 32.0, 29.8, 29.7, 29.6, 29.4, 28.9, 26.3, 22.8, 15.0, 14.2. MS (FAB): m/z 70 (7 %, TrH^+), 98 (11 %, $K^+-C_{12}H_{24}$), 266 (100 %, K^+),406 (32 % $K^+ - C_2H_5 + C_{12}H_{25}$). Elemental analysis (%) calcd for ($C_{16}H_{32}N_3Br$): C 55.48, H 9.31, N 12.13; found: C 55.78, H 10.02, N 11.63.

1-DODECYL-3-METHYL-1,2,3-TRIAZOLIUM BROMIDE (10)
^{1}H NMR (200 MHz, $CDCl_3$) δ: 9.77 (d, J = 1.2 Hz, 1H), 9.61 (d, J = 1.3 Hz, 1H), 4.74 (t, J = 7.4 Hz, 2H), 4.54 (s, 3H), 2.04 (t, J = 7.2 Hz, 2H), 1.36 – 1.22 (m, 18H), 0.87 (t, J = 6.4 Hz, 3H). ^{13}C NMR (50 MHz, $CDCl_3$) δ: 132.6, 131.7, 54.3, 40.7, 32.0, 29.8, 29.7, 29.6, 29.4, 28.9, 26.2, 22.8, 14.2. MS (FAB): m/z 84 (14 %, $K^+-C_{12}H_{24}$), 252 (100 %, K^+), 406 (1.3 %, $K^+ - CH_3 + C_{12}H_{25}$), 583 (22 %, $2*K^+ + Br^-$). Elemental analysis (%) calcd for ($C_{15}H_{30}N_3Br$): C 54.12, H 9.1, N 12.64; found: C 53.06, H *10.01*, N 12.24.

Instrumentation

Differential scanning calorimetry (DSC) was performed with a computer-controlled PhoenixDSC 204 F1 thermal analyzer (Netzsch, Selb, Germany). Measurements were carried out at a heating rate of 5 °C/min in sealed aluminium crucible with an argon flow rate of 20 mL/min. The samples were placed in aluminium pans which were cold-sealed. Reported temperatures correspond to the onset of the respective thermal process.

Optical analyses were made by heated-stage polarized optical microscopy (POM) with an Axio Imager A1 microscope (Carl Zeiss MicroImaging GmbH,Göttingen, D) equipped with a hot stage, THMS600 (Linkam ScientificInstruments Ltd, Surrey, UK), and Linkam TMS 94 temperature controller (Linkam Scientific Instruments Ltd, Surrey, UK). Images were recorded at a magnification of 100× as a video with a digital camera during heating and cooling the sample which was places between two cover slips. Heating and cooling rates were 5 °K/min[-1].

Temperature-dependent SAXS experiments (compound **1-9**) were carried out at the BW4 Beamline of DORIS III, Hasylab (DESY, Hamburg, Germany) at a fixed wavelength of 1.38 Å. The data were collected with a MarCCD detector. The detector was calibrated with silver behenate and the sample–detector position was fixed at 455 mm. For measurements, the samples

were placed between aluminum foil in a copper sample holder, the sample chamber was evacuated and the temperature was controlled via a JUMO IMAGO 500 multi-channel process and program controller. The program "a2tool" (Hasylab) was used for data reduction, analysis and correction. The SAXS-data for compound 10 were collected with a D8 Advance diffractometer (Bruker) with molybdenum source (λ = 0.71073 Å).

Powder-XRD measurements were carried out at a HUBER G670 diffractometer with molybdenum source. The samples were filled in a class capillary with a diameter of 0.5 mm. For high temperature measurements a U-shaped ceramic heating fork was placed above the capillary. The temperature was regulated via a high temperature controller HUBER HTC 9634.

Crystals of 1,3-didodecyl-1,2,3-triazole bromide (**2**) were obtained from recrystallization of the compound in cold dichloromethane. This data were collected on a Rigaku XTaLAB mini diffractometer (with graphite monochromated Mo Kα radiation, λ = 0.71073 Å) at 170 K. Single Crystals of 1-dodecyl-3-methyl-1,2,3-triazolium bromide ($[C_{12}C_1Tr][Br]$,(**10**)) could be grown successfully from a dichloromethane solution. Single crystals of sufficient quality for structure analysis of compound no. **7** ($[C_{12}C_5Tr][Br]$) where grown by melting the substance and very slowly cooling it to room temperature. Measurements were carried out on a Stoe IPDS-I single-crystal X-Ray diffractometer with graphite monochromated Mo Kα radiation (λ = 0.71073 Å at 100 K). Crystal structure solution by direct methods using SIR 92[37] yielded the heavy atom positions. Refinement with SHELXL-97[38] allowed for the localization of the remaining atom positions. Hydrogen atoms were added and treated with the riding atom mode. Data reduction was performed with the program package X-Red[39] and numerical absorption correction was carried out with the program X-Shape[40]. To illustrate the crystal structures, the program Diamond[41] was used.

Acknowledgements

Notes and references

^{a}*Anorganische Chemie III – Materials Engineering and Characterization, Fakultät für Chemie und Biochemie,Ruhr-Universität Bochum, 44780, Bochum, Germany.*
^{b}*Materials Science and Engineering, Iowa State University and Critical Materials Institute, Ames Laboratory, Ames, UA, USA*

† Electronic Supplementary Information (ESI) available: [SAXS and PXRD]. See DOI: 10.1039/b000000x/

1 Wasserscheid, P.; Welton T. (Eds.), *Ionic Liquids in Synthesis*, Wiley-VCH, Weinheim, Germany, **2003**

2 Plechkova, N. V.; Seddon, K. R. *Chem. Soc. Rev.* **2008**, *37*, 123.

3 Freemantle, M. *Chem. Eng. News* **1998**, *76*, 32–37.

4 Wilkes, J. S. *Green Chem*, **2002**, 4, 73

5 Welton, T. *Chem. Rev.*, **1999**, 99 (8), 2071–2084; Boroqqs, E.; Earle, M.-J.; Gilea, M.-A.; Metlen, A.-; Mudring, A.-V.; Rieger, F.; Robertson, A.J.; Seddon, K.-R.; Tomaszowska, A.A.; Trusov, L.; Vyle; J.S., *Chem. Commun.*, **2010**, *46*, 716-718

6 Richter, K.; Bäcker, T.; Mudring, A.-V., *Chem.Commun.*, **2009**, 301-303; Prondzinski, N.-V.; Cybinska, J.; Mudring, A.-V. *Chem. Commun.*, **2010**, *46*, 4393- 4395; Lorbeer, C. Cybinska, J. Mudring, A.-V, *Chem. Commun.*, **2010**, *46*, 571-573; Richter, K.; Birkner, A.; Mudring, A.-V. *Angew. Chem. Int. Ed.*, **2010**, *49*, 2431-2435; Richter, K.; Birkner, A.; Mudring, A.-V., *Phys. Chem. Chem. Phys.*, **2011**, *13*, 7136–7141; Lorbeer, C. Cybinska, J. Mudring, A.-V *Cryst. Growth Des.,* **2011**, *11*, 1040-1048; Lorbeer, C. Cybinska, Zych, G.; Mudring, A.-V., *ChemSusChem*, **2011**, *4*, 595-598; Alammar, T.; Mudring, A.-V.:, *ChemSusChem*, **2011**, *12*, 1796-1804 Lorbeer, C. Cybinska, Zych, G.; Mudring, A.-V., *ChemSusChem*, **2011**, *4*, 595-598; Alammar, T.; Shekhah, O.; Mudring, A.-V., *J. Mater. Chem.*, **2012**, *22*, 18252-18260.Lorbeer, C. Cybinska, J. Mudring, A.-V. , *J. Mater. Chem.,* **2012**, *22*, 9505-9508.; Campbell, P. S. Lorbeer, C. Cybinska, J. Mudring, A.-V. *Adv. Funct. Mater.*, **2013**, *23*, 2924-2931.; Lorbeer, C.; Mudring, A.-V., *J. Phys. Chem. C*, **2013**, 12229-12238.; Lorbeer, C.; Mudring, A.-V., *ChemSusChem*, **2013**, *6*, 2382-2387; Alammar, T.; Noei, H.; Wang, Y.; Mudring, A.-V.; *Nanoscale*, **2013**, *5*, 8045-8055.Lorbeer, C. Cybinska, J.; Mudring, A.-V.*J. Mat. Chem. C*, **2014**, 2, 1862-1868; Yang, M.; Campbell, P.; Santini, C.; Mudring, A.-V., *Nanoscale*, **2014**, *6*, 3367-3375.

7 O'Reagan, B.; Grätzel, M. *Nature* **1991**, 353, 737.

8 Endres, F.; MacFarlane, D.; Abbott A. (Eds.), *Electrodeposition from ionic liquids*, Wiley-VCH, Weinheim, Germany, **2008**.

9 Axenov, K. V.; Laschat, S. *Materials* **2011**, 4, 206-259.

10 Bowlas, C.J.; Bruce, D.W.; Seddon K.R. *Chem. Commun.* **1996**, *14*, 1625-1626.

11 Taguchi, S.; Ichikawa, T.; Kato, T.; Ohno H. *Chem Commun.* **2012,** 48, 5271–5273.

12 Lee, K. W.; Lee, C. K.; Lin, I. J. B. *Chem. Commun.* **1997**, 899.

13 Bradley, A. E.; Hardacre, C.; Holbrey, J. D.; Johnston, S.; McMath, S. E. J.; Nieuwenhuyzen, M. *Chem. Mater.* **2002***, 14, 629-635;* Getsis, A. Mudring A.-V.: *Acta Cryst.* **2005**, *E61*, o2945-o2946 Getsis, A.

Mudring A.-V., *Cryst. Res. Technol.*, **2008**, *43*, 1187-1196; Yang, M. Stappert, K.; Mudring, A.-V., *J. Mat. Chem. C*, **2014**, *2*, 458-473;

14 Lava, K.; Binnemans, K.; Cardinaels, T. *J. Phys. Chem. B* **2009**, 113, 9506-9511.

15 Getsis, A.; Mudring, A.-V. *Z. Anorg. Allg. Chem.* **2009**, 635, 2214-2221.

16 Goossens, K.; Lava, K.; Nockemann, P.; Van Hecke, K.; Van Meervelt, L.; Driesen, K.; Görller-Walrand, C.; Binnemans, K.; Cardinaels, T. *Chem. Eur. J.* **2009**, 15, 656-674.

17 Ma, K.; Lee, K.-M.; Minkova, L.; Weiss, R.G. *J. Org. Chem.* **2009**, *74*, 2088-2098.

18 Li, X.; Bruce, D.W.; Shreeve, J.M. *J. Mater. Chem.* **2009**, *19*, 8232-8238.

19 Zeng, Z.; Phillips, B. S.; Xiao, J.-C.; Shreeve, J. M. *Chem. Mater.* **2008**, *20*, 2719–2726.

20 Yang, M.; Stappert, K.; Mudring, A.-V. *J. Mater.Chem. C* **DOI:** 10.1039/C3TC31368A

21 Downard, A.; Earle, M.J.; Hardacre, C.; McMath, S.E.J.; Nieuwenhuyzen, M.; Teat, S.J. *Chem. Mater.* **2004**, *16*, 43-48.

22 Holbrey, J.D.; Seddon, K. R. *J. Chem. Soc., Dalton Trans.* **1999**, *13*, 2133-2139.

23 Getsis, A.; Mudring, A.- V. *Cryst. Res. Technol.* **2008**, 43, 1187

24 Wang, X.; Vogel, C. S.; Heinemann, F. W.; Wasserscheid, P.; Meyer, K. *Cryst. Growth Des.* **2011**, *11*, 1974–1988.

25 Luo, S.-C.; Sun, S.; Deorukhkar, A. R.; Lu, J.-T.; Bhattacharyya, A.; Lin, I. J. B. *J. Mater. Chem.*, **2011**, *21*, 1866–1873.

26 Dobbs, W.; Douce, L.; Allouche, L.; Louati, A.; Malbosc, F.; Welter, R. *New J. Chem.* **2006**, 30, 528 – 532.

27 Getsis, A.; Balke, B.; Felser, C.; Mudring, A.-V.*, Cryst. Growth Des.*, **2009**, *9*, 4429-4437; Getsis, A. ; Mudring, A.-V. *Z. Allg.Anorg.Chem.*, **2010**, *636*, 1726-1734; Getsis, A. ; Mudring, A.-V., *Eur. J. Inorg. Chem.*, **2010**, *14,* 2172-2177; Getsis, A. ; Mudring, A.-V.**,** *Eur. J. Inorg. Chem.,* **2011**, *21*, 3207–3213; Bäcker, J.; Mihm, S.; Mallick, B.; Yang, M.; Meyer, G.; Mudring, A.-V. *Eur. J. Inorg.Chem.*, **2011**, *26*, 4089-4095; Campbell, P.; Yang, M.; Cybinska, J. Pitz, D.; Mudring, D., *Chem. Eur. J.*, **2014**, *20*, 4704-4712.

28 Yamanaka, N.; Kawano, R.; Kubo, W.; Masaki,N.; Kitamura, T.; Wada, Y.; Watanabe, M.; Yanagida, S. *J. Phys. Chem. B* **2007**, 111, 4763-4769

29 Kohler,F. T. U.; Morain,B.; Weiß,A.; Laurin, M.; Libuda,J.; Wagner,V.; Melcher, B. U.; Wang, X.; Wasserscheid, P.; Meyer, K. *ChemPhysChem* **2011**, 12, 3539 – 3546.

30 Chowdhury,S.; Mohan, R. S.; Scott, J. L. *Tetrahedron* **2007**, 2363–2389.

31 Jeong, Y. ; Ryu, J.-S. *J. Org. Chem.***2010**, 75, 4183–4191.

32 Stappert, K.; Ünal, D.; Mallick, B.; Mudring, A.-V. *J. Mater. Chem. C,* **2014**, Accepted Manuscript **DOI:** 10.1039/C3TC31366B

33 Mudring, A.-V. *Aust. J. Chem.*, **2010**, *63*, 544-564.

34 Yang, M.; Mallick,B.; Mudring, A.-V. *Cryst. Growth Des.*, **2013**, *13* (7), 3068–3077.

35 Yang, M. ; Mallick, B.; Mudring, A.-V. *Cryst. Growth Des.* **2014**, *14*, 1561 −1571.

36 Juríček, M. ; Kouwer, P. H. J. ; Rehák, J. ; Sly, J. ; Rowan, A. E. *J. Org. Chem.*, **2009**, 74 (1), 21–25.

37 SIR-92: Altomare, A.; Cascarano, G.; Giacovazzo, G. *J. Appl.Crystallogr.* **1993**, *26*, 343.

38 Sheldrick, G. M. *SHELXL-97*, Programs for Crystal Structure Analysis, University of Göttingen, Germany, **1997**.

39 *X-RED*, v. 1.22, Stoe Data Reduction Program (C), Stoe & Cie GmbH, Darmstadt, Germany, **2001**;

40 *X-Shape*, v. 1.06, Crystal Optimisation for Numerical Absorption Correction (C), Stoe & Cie GmbH, Darmstadt, **1999.**

41 Brandenburg, K.; Putz, H. *DIAMOND*, Program for Crystal and Molecular Structure Visualization, Crystal Impact GbR, Bonn, Germany.

RSC Advances Accepted Manuscript